Reversible Addition of CO to Unsaturated High-Spin Iron(II) Complexes: Evidence of the First Octahedral High Spin Iron(II) Dicarbonyl Complex

Christian Holzhacker,[†] Christina M. Standfest-Hauser,[†] Michael Puchberger,[‡] Kurt Mereiter,[§] Luis F. Veiros,[∥] Maria José Calhorda,[⊥] Maria Deus Carvalho,[≠] Liliana P. Ferreira,[#,¶] Margarida Godinho,[#] Frantisek Hartl,[€] and Karl Kirchner*,[†]

Supporting Information

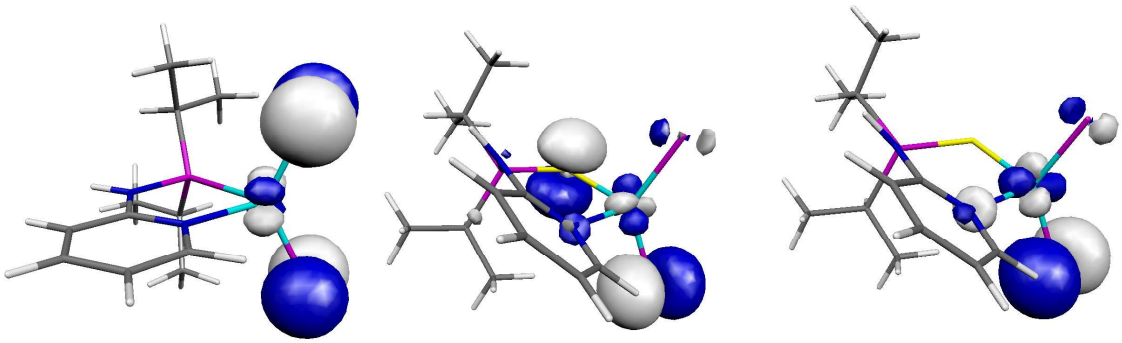

5a **8a** **9**

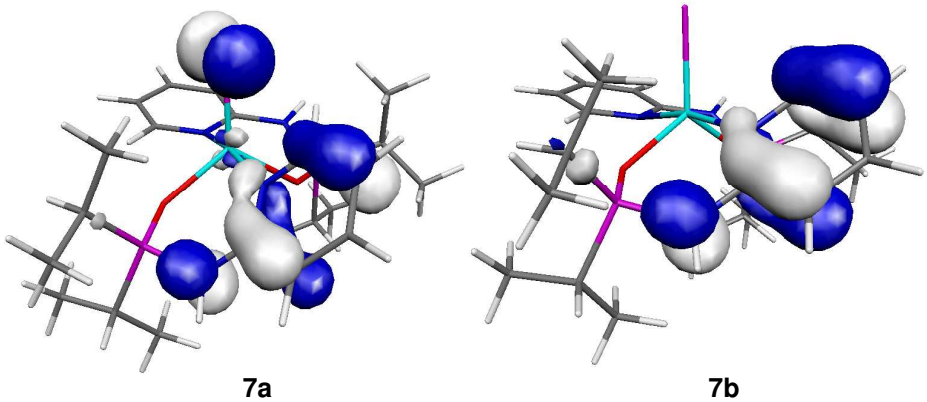

7a **7b**

Figure S1. The β electron orbital for each of the five complexes [Fe(PN-*i*Pr)Cl_2 (**5a**), [Fe(SN-*i*Pr)Cl_2 (8a), [Fe(SeN-*i*Pr)Cl_2 (**9**), [Fe(ON-*i*Pr)$_2$Cl]Cl (**7a**), and [Fe(ON-*i*Pr)$_2$Br]Br (**7b**)

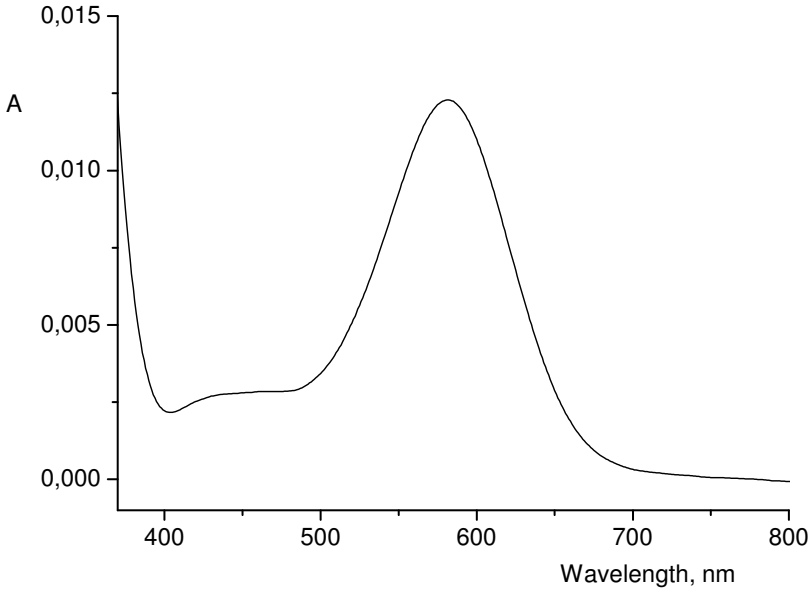

Figure S2. Difference absorbance UV-Vis spectrum of [Fe(PN-*i*Pr)Br_2] (**5b**) in CO-saturated CH_2Cl_2 at -50 °C (λ_{max} = 584 nm).

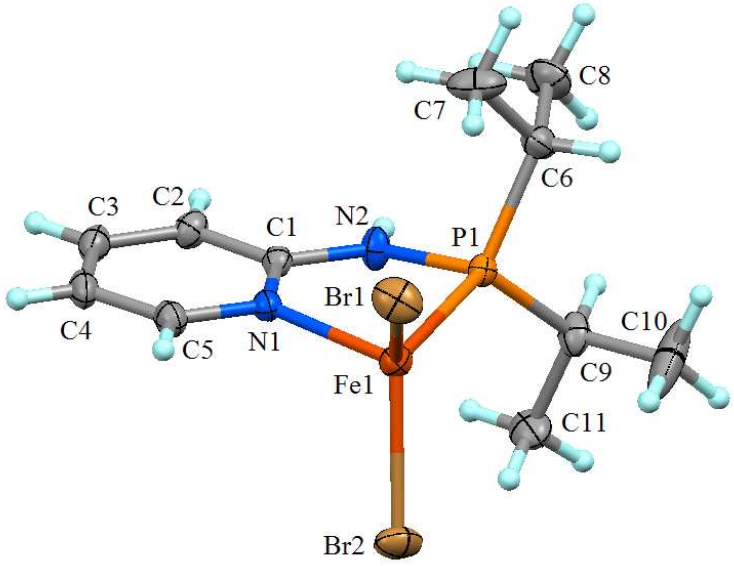

Figure S3. Structural diagram of [Fe(PN-*i*Pr)Br_2] (**5b**) showing 50% displacement ellipsoids. Selected distances and angles (Å, °): Fe1–N1 2.0995(14), Fe1–P1 2.4277(6), Fe1–Br1 2.3643(4), Fe1–Br2 2.3974(4), P1–N2 1.702(2), N2-C1 1.379(2), N1–Fe1–P1 80.74(4), N1–Fe1–Br1 110.86(4), N1–Fe1–Br2 105.71(4), P1–Fe1–Br1 121.97(2), P1–Fe1–Br2 110.86(2), Br1–Fe1–Br2 118.80(2), Fe1–P1–N2 96.22(5), P1-N2-C1 122.9(1), N1-C1–N2–P1 8.8(2), C1–N2–P1–Fe1 4.0(2); hydrogen bond N2···Br2 3.429(2) not shown. [Fe(PN-*i*Pr)Br_2] (**5b**) is not isostructural with the chloride homologue [Fe(PN-*i*Pr)Cl_2] (**5a**).

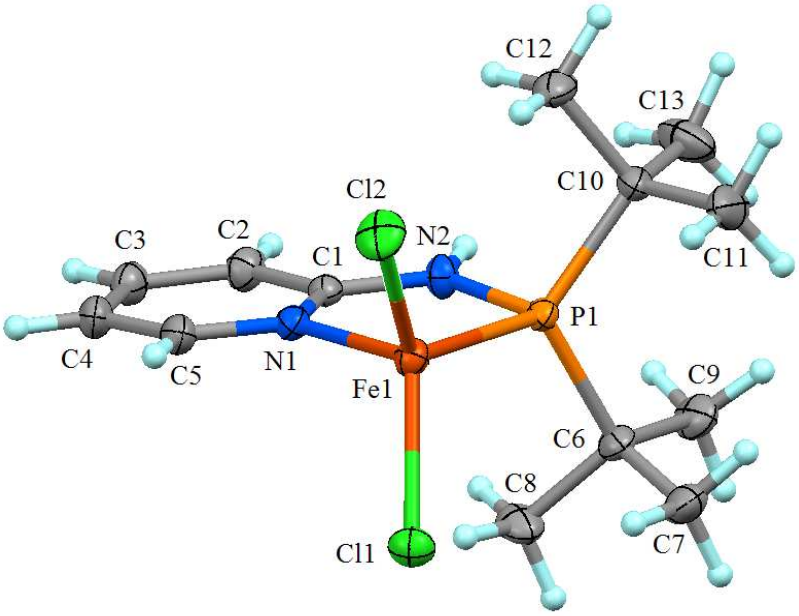

Figure S4. Structural diagram of [Fe(PN-*t*Bu)Cl_2] (**6a**) showing 50% displacement ellipsoids. Selected distances and angles (Å, °): Fe1–N1 2.0978(12), Fe1–P1 2.4249(4), Fe1–Cl1 2.2624(4), Fe1–Cl2 2.2336(4), P1–N2 1.7032(13), N2-C1 1.3848(17), N1–Fe1–P1 80.39(4), N1–Fe1–Cl1 111.17(4), N1–Fe1–Cl2 108.57(4), P1–Fe1–Cl1 112.53(2), P1–Fe1–Cl2 122.79(2), Cl1–Fe1–Cl2 115.37(2), Fe1–P1–N2 97.71(4), P1-N2-C1 121.74(10), N1-C1–N2–P1 7.14(18), C1–N2–P1–Fe1 -7.49(12); hydrogen bond N2···Cl1 3.314(1) not shown.

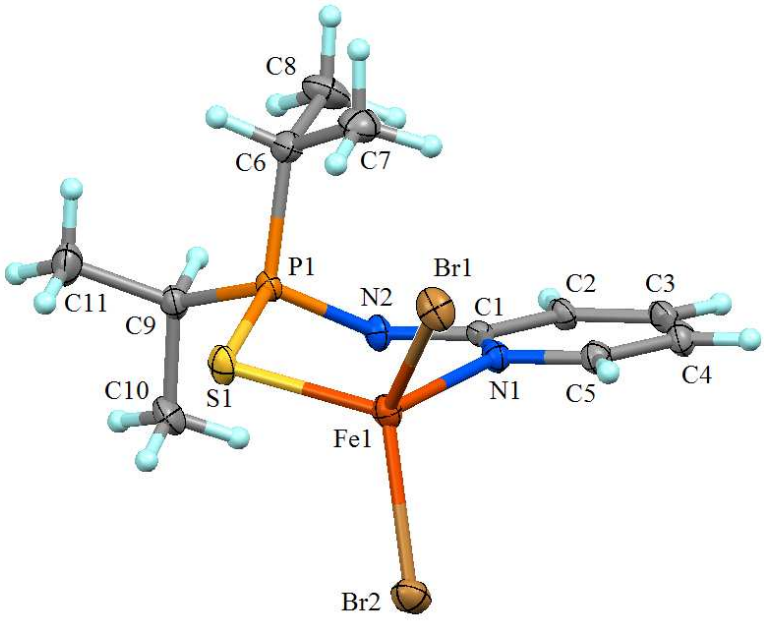

Figure S5. Structural diagram of [Fe(SN-*i*Pr)Br_2] (**8b**) showing 50% displacement ellipsoids. Selected distances and angles (Å, °): Fe1–N1 2.121(2), Fe1–S1 2.3654(6), Fe1–Br1 2.4264(4), Fe1–Br2 2.3887(4), P1–S1 1.9934(7), P1–N2 1.682(2), N2–C1 1.398(2), N1–Fe1–S1 104.19(5), N1–Fe1–Br1 100.91(5), N1–Fe1–Br2 106.32(5), S1–Fe1–Br1 113.11(2), S1–Fe1–Br2 112.78(29), Br1–Fe1–Br2 117.57(2), Fe1–S1–P1 99.88(2), S1-P1-N2 114.36(7), N1-C1–N2–P1 40.9(3), C1–N2–P1–S1 -67.1(2), N2–P1–S1–Fe1 34.25(7); hydrogen bond N2···Br1 3.444(2) not shown, the hydrogen atom bonded to N2 is hidden behind N2. Compounds [Fe(SN-*i*Pr)Cl_2] (**8a**), [Fe(SN-*i*Pr)Br_2] (**8b**), and [Fe(SeN-*i*Pr)Cl_2] (**9**) form an isostructural series.

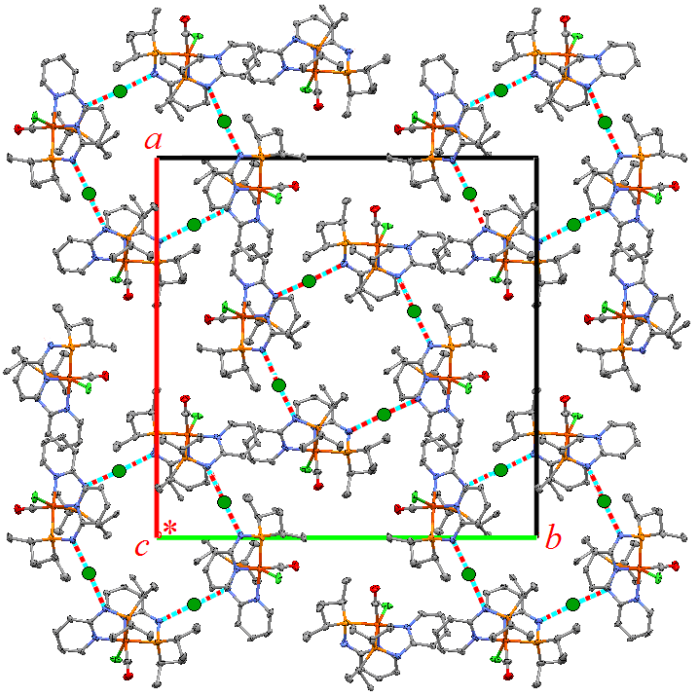

Figure S6. Packing diagram of [Fe(PN-*i*Pr)$_2$(CO)Cl]Cl.*solv* (**10a**), which crystallizes in the tetragonal space group $I\bar{4}$ (no. 82) and features hydrogen bonded cyclic tetramers (dashed lines) of [Fe(PN-*i*Pr)$_2$(CO)Cl]$^+$ cations and chloride anions (green dots). Disordered solvent is located in channels parallel to *z* at *x*,*y* = 0,0; ½,0; etc.